# Semi-exclusive cross sections for charged-current quasi elastic and neutral-current elastic neutrino scattering off $^{40}$Ar and a sterile neutrino oscillation study

A. Butkevich

INR RAS, Moscow

XXXV International Workshop on HEP, IHEP, November 30, 2023

- (⋆) The discovery and study of neutrino oscillations have increaset interest in neutrino-nucleus interactions
- (⋆) All data of long-baselane neutrino experiments with solar, reactor, atmospheric and accelerator experiments can be described within the 3-flavor model of neutrino oscillation with the three active neutrinos $\nu_e, \nu_\mu$, and $\nu_\tau$ predicted by the Standard Model.
- (⋆) On the other hand, during the last decades, a few of anomalous of neutrino oscillation measurements ("gallium", "reactor" anomalies, LSND and MiniBooNE accelerator neutrino experiments) have been made at short baseline.
- (⋆) Data from these short-baseline (at distance less then 1km between neutrino source and detector) hint at the existence of additional eV-scale neutrino mass states $\nu_s$ beyond the three active species in the Standard Model $\nu_{active} = \nu_e, \nu_\mu, \nu_\tau$
- (⋆) "Sterile neutrino" $\nu_s$ has no coupling to either the $W^\pm$ or $Z^0$ bosons.

- (⋆) The simplest extension to this 3-flavor model is referred as the 3+1 model and introduces a single new mass state, with a corresponding sterile flavor state $\nu_s$ and $m_4(\approx 1\ eV) >> m_1, m_2, m_3$.
- (⋆) The effects of $\nu_\mu$ disappearance and $\nu_e$ appearance in muon neutrino beam are detected in $\nu_\mu(\nu_e)$ charged current (CC) $\nu A$ interactions and the effect of any active neutrino disappearance $\nu_{active} \rightarrow \nu_s$ is detected in NCE $\nu A$ scattering.

## Experiment

- (⋆) The Short-Baseline Neutrino program (SBN) hosted at Fermilab was proposed for a definitive resolution to the short-baseline anomalies.
- (⋆) SBN consists of three hundred ton scale liquid argon time-projected chambers (LArTPC) located along the Booster Neutrino beam (BNB) axis at distances hundreds meters from the BNB target; a near detector SBND; an intermediate detector MicroBooNE; and a far detector ICARUS.

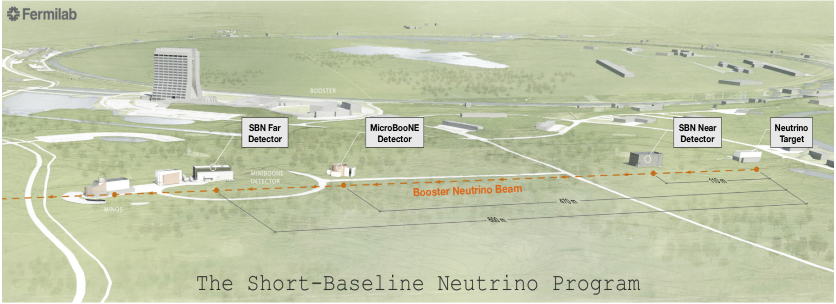


Layout of the SBN program at Fermilab. Three large LArTPC will site along BNB, that created by 8 GeV proton from Booster accelerator

- (⋆) SBND is near detector a 112 ton will be located at 110 m down strem from the BNB target
- (⋆) ICARUS-T600 is far detector a 470 ton at distance 600 m from the BNB target
- (⋆) MicroBooNE is intermediate detector a 85 ton located 469 m from BNB target along the beam.
- (⋆) The composition of the flux in $\nu_\mu$ mode at near(far) detector 97.5% $\nu_\mu$, 1.8%(1.6%) $\bar{\nu}_\mu$, 0.7%(0.6%) $(\nu_e + \bar{\nu}_e)$

(⋆) The flux-integrated semi-exclusive charged current (CC) quasielastic (QE)

$$\nu_\mu + {}^{40}Ar \rightarrow \mu + p + B$$

and neutral current elastic

$$\nu_\mu + {}^{40}Ar \rightarrow \nu_\mu + p + B$$

cross sections were measured in MicroBooNE experiment.

(⋆) These cross sections were calculated with the relativistic distorted-wave impulse approximation (RDWIA), using the BNB flux. We calculated cross sections as functions of reconstructed neutrino energy.

(⋆) Possible application of these cross sections, calculated for near SBND and far ICARUS detectors for sterile neutrino search at SBN is study.

# Formalism of the CCQE and NCE scattering

## CCQE and NCE exclusive reactions

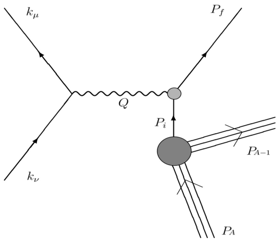


$l(k_i) + A(p_A) \to l'(k_f) + N(p_x) + B(p_B)$,
where $q = (\omega, \mathrm{q}) = k_i - k_f$ и $Q^2 = -q^2$.

Impulse approximation
$W/Z$-bozon interacts only with one nucleon with production one particle - one hole $(1p - 1h)$ in a final state.

Differential cross sections for the exclusive CCQE and NCE scattering in which only a single discrete state or narrow resonance of the target is excited can be written as

$$\frac{d^5\sigma^{(nc)}}{d\varepsilon_f d\Omega_f d\Omega_x} = R\frac{|\mathbf{p}_x|\varepsilon_x}{(2\pi)^5}\frac{|\mathbf{k}_f|}{\varepsilon_i}\frac{\tilde{G}^{2(cc)(nc)}}{2}L^{(nc)}_{\mu\nu}W^{\mu\nu(nc)},$$

where $\Omega_f = (\theta, \varphi)$ is the solid angle for lepton scattering, $\Omega_x = (\theta_x, \phi)$ is the solid angle for the ejectile nucleon momentum, $\tilde{G}^{(cc)} = M_W^2 G\cos\theta_c/(Q^2 + M_W^2)$, $\tilde{G}^{(nc)} = M_Z^2 G/(Q^2 + M_Z^2)$ and $G \simeq 1.16639 \times 10^{-11}$ MeV$^{-2}$ is the Fermi constant, $\theta_C$ is the Cabbibo angle ($\cos\theta_C \approx 0.9749$), $L^{(cc)(nc)}_{\mu\nu}$ is CC(NC) current lepton tensor, and $W^{\mu\nu(cc)(nc)}$ is weak hadron tensors of charged (neutral) current and $R$ is a recoil factor.

All the nuclear structure information and final state interaction effects are contained in weak CC and NC nuclear tensors $W^{(cc)(nc)}_{\mu\nu}$

$$W^{(cc)(nc)}_{\mu\nu} = \sum\langle B_f, p_x|J^{(cc)(nc)}_{\mu}|A\rangle\langle A|J^{(cc)(nc)}_{\nu}|B_f, p_x\rangle,$$

$J_\mu$ is the nuclear CC(NC) operator, and $|A\rangle$ and $|B_f, p_x\rangle$ are the initial and final states, respectively of the hadron system. Sum is taken over undetected states $|B_f\rangle$.

General expressions for the cross sections of exclusive CCQE and NCE neutrino scattering of nucleus are given in terms of nuclear response function $R_i^{(cc)(nc)}$

$$\frac{d^5\sigma^{(cc)(nc)}}{d\varepsilon_f d\Omega_f d\Omega_x} = \frac{|\mathbf{p}_x|\varepsilon_x}{(2\pi)^5} G^{2(cc)(nc)} \varepsilon_f |\mathbf{k}_f| R$$
$$\times \{ v_0 R_0^{(cc)(nc)} + v_T R_T^{(cc)(nc)} + v_{TT} R_{TT}^{(cc)(nc)} \cos 2\phi$$
$$+ v_{zz} R_{zz}^{(cc)(nc)} + (v_{xz} R_{xz}^{(cc)(nc)} - v_{0x} R_{0x}^{(cc)(nc)}) \cos\phi$$
$$- v_{0z} R_{0z}^{(cc)(nc)} + h [ v_{yz} (R_{yz}'^{(cc)(nc)} \sin\phi + R_{yz}^{(cc)(nc)} \cos\phi)$$
$$- v_{0y} (R_{0y}'^{(cc)(nc)} \sin\phi + R_{0y}^{(cc)(nc)} \cos\phi) - v_{xy} R_{xy}^{(cc)(nc)} ] \}.$$

The response functions $R_i$ are suitable combinations of the hadron tensor $W_{ij}$ components, for example,

$$R_0^{(cc)(nc)} = W^{00(cc)(nc)}, \quad R_T^{(cc)(nc)} = W^{xx(cc)(nc)} + W^{yy(cc)(nc)}, \quad ...$$

and depend upon $(Q^2, \omega)$ or $(|\mathbf{q}|, \omega)$, and coefficients $v_i$ depend upon lepton kinematic A.Butkevich PRC 76,045502 (2007).

The exclusive cross section of the CCQE scattering as a function of $\varepsilon_f$ and $\cos\theta$ can be written as

$$\frac{d^3\sigma}{d\varepsilon_f d\Omega_f} = \int_0^{2\pi} d\phi \int dp_m R_c \frac{d^5\sigma}{d\varepsilon_f d\Omega_f d\Omega_x},$$

where

$$R_c = \frac{p_m}{p_x|q|}\left[1 + \frac{\varepsilon_x}{2p_x\varepsilon_B}(p_x^2 + |q|^2 - p_m^2)\right]$$

As the outgoing neutrino is undetected the differential cross section of the NCE interaction in the "target nucleon at rest" approximation as a function of $(p_x, \cos\theta_p)$ can be written as

$$\frac{d\sigma^2}{dp_x d\cos\theta_p} \approx R_p \frac{d^2\sigma}{d\varepsilon_f d\cos\theta},$$

where $R_p = p_x^2/[\varepsilon_x(\varepsilon_i - \omega)]$.

# RDWIA Model

## Relativistic distorted-wave impulse approximation (RDWIA)

(∗) We describe the lepton-nucleon scattering in the Impulse Approximation (IA), in which only one nucleon of the target is involved in reaction. This approximation can be used at $|q| > 200$ MeV.

(∗) The nuclear current is written as the sum of single-nucleon currents $J^\mu_A = \sum_i j^\mu_i$.

(∗) Then the nuclear matrix element take form.

$$\langle p, B|J^\mu|A\rangle = \sum \int d^3r\ \exp(i\mathbf{t}\cdot\mathbf{r})\overline{\Psi}^{(-)}(\mathbf{p},\mathbf{r})\Gamma^\mu\Phi(\mathbf{r}),$$

where $\Gamma^\mu$ is the vertex function, $\Phi$ and $\Psi^{(-)}$ are relativistic bound-state and outgoing nucleon wave functions, $t = \varepsilon_B|q|/W$ is the recoil-corrected momentum transfer, $W = [(m_A + \omega)^2 - q^2]^{1/2}$ is the invariant mass.

- Sing-nucleon charged-current

has V-A structure $J^{\mu(cc)} = J_V^{\mu(cc)} + J_A^{\mu(cc)}$. For free nucleon vertex function $\Gamma^{\mu(cc)} = \Gamma_V^{\mu(cc)} + \Gamma_A^{\mu(cc)}$, we use CC2 vector function

$$\Gamma_V^{\mu(cc)} = F_V^{(cc)}(Q^2)\gamma^\mu + i\sigma^{\mu\nu}\frac{q_\nu}{2m}F_M^{(cc)}(Q^2),$$

$\sigma_{\mu\nu} = i[\gamma^\mu\gamma^\nu]/2$, $F_V$ и $F_M$ - the weak vector form factors are related to the corresponding electromagnetic ones for protons $F_{i,p}^{(el)}$ and neutrons $F_{i,n}^{(el)}$ (CVC) as $F_i = F_{i,p}^{(el)} - F_{i,n}^{(el)}$, where $i = V, M$.

- The axial current vector function is related to the axial $F_A$ and pseudoscalar $F_P$ form factors as

$$\Gamma_A^\mu = F_A^{(cc)}(Q^2)\gamma^\mu\gamma_5 + F_P^{(cc)}(Q^2)q^\mu\gamma_5.$$

The axial and pseudoscalar form factors in the dipole approximation are parametrized as
$F_A^{(cc)}(Q^2) = F_A^{(cc)}(0)/(1 + Q^2/M_A^2)^2, F_p(Q^2) = 2mF_A(Q^2)/(m_\pi^2 + Q^2)$
where $F_A(0) = 1.267$ and $1 < M_A < 1.2$ GeV is the axial mass of nucleon.

- Sing-nucleon neutral current.

$$\Gamma_V^{\mu(nc)} = F_V^{(nc)}(Q^2)\gamma^\mu + i\sigma^{\mu\nu}\frac{q_\nu}{2m}F_M^{(nc)}(Q^2),$$

where the vector form factors of vector current

$$F_V^{(nc)} = \tau_3(0.5 - \sin^2\theta_W)(F_1^p - F_1^n) - \sin^2\theta_W(F_1^p + F_1^n) - F_V^s/2$$
$$F_M^{(nc)} = \tau_3(0.5 - \sin^2\theta_W)(F_2^p - F_2^n) - \sin^2\theta_W(F_2^p + F_2^n) - F_M^s/2,$$

$\tau_3 = +(-1)$ for proton(neutron) $p(n)$ и $\theta_W$ is Weinberg angle.

- The neutral current vertex function are related to the axial form factor as

$$\Gamma_A^{(nc)} = (\tau_3 F_A + F_A^S)/2,$$

where a contribution of the strange quarks to the neutral-current axial form factor in dipole approximation is parametrized as

$$F_A^S = \Delta s/(1 + Q^2/M_A^2)^2$$

with $F_A(0) = 1.272$ and $\Delta s$ describes the possible strange-quark contribution. We use the MMD approximation *P. Mergell et al. Nucl.Phys. A596, 367 (1996)* of vector nucleon form factors and neglect the possible strange-quark contribution. In this calculation we neglect this contribution, i.e. $F_V^S = F_M^S = 0$.

# Модель

(⋆) In the RDWIA approach the IPSM is used in the calculations of the nuclear structure of the target. The relativistic bound-state functions for nucleon $\Phi$ are obtained as the self-consistent solutions of the Dirac equations for nucleon, derived within a relativistic mean-field approach from Lagrangian containing $\sigma, \omega$ and $\rho$ mesons *C.J. Horowits et al. Nucl.Phys A368, 503 (1981)*

- ⋆ These functions were calculated by the TIMORE code *C.J. Horowitz at al. 1991* with the normalization factors $S_\alpha$ relative to full occupancy of the IPSM orbital $\alpha$ of $^{40}$Ca.
- ⋆ For $^{40}$Ca and $^{40}$Ar an average factor $< S > \approx 87$%. This estimation of depletion of hole states follows from the RDWIA analysis of $^{40}$Ca data *A. Butkevich PRC85, 065501 (2012)* *G.J.Kramer Ph.D. thesis (1991), G.J. Kramer et al. Phis.Lett.B227(1989)199*.
- ⋆ We assume that missing strength (13%) can be attributed the short-range nucleon correlations in ground state, leading to the appearance of the high-momentum and high-energy component in the nucleon distribution in the target.

In the RDWIA final state interaction effects for the outgoing nucleons are taking into account. The ejectile wave function $\psi$ is solution of a Dirac equation containing the scalar and vector potentials $S$ and $V$, that are energy dependent.

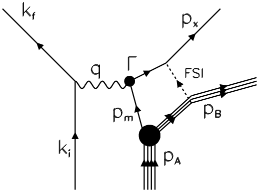


$$[\boldsymbol{\alpha} \cdot \mathbf{p} + \beta(m + S)]\, \psi = (E - V)\psi,$$

$$\psi(\mathbf{r}) = \begin{pmatrix} \psi_+(\mathbf{r}) \\ \psi_-(\mathbf{r}) \end{pmatrix}$$

We use the LEA code *J.J. Kelly (1995)* for numerical calculation of the distorted wave functions with EDAD1 SV approximation of the relativistic optical potential *E.D. Cooper et al. (1993)*.

The optical potential consists of a real part, which describes the rescattering of the ejected nucleon and an imaginary part which account for its absorption into unobserved channels.

The RDWIA approach was successfully tested against Ca$(e, e'p)$ and Ca(Ar)$(e, e')$ data A.Bukevich, PRC 85,065501 (2012); PRC 102,024602 (2020).

⋆ The measurement of exclusive CCQE-like cross sections was performed using the MicroBooNE detector P. Abratenko et al. PRL 125, 201803 (2020)
A subset of CCQE-like interaction (CC1p0$\pi$) includes

$$\nu_\mu + {}^{40}Ar \rightarrow \mu + p + B,$$

events with a detected muon with $p_\mu > 100$ MeV/c and exactly one proton with $\mathbf{p}_p > 300$ MeV/c and no pion.
⋆ Selected (CC1p0$\pi$) event definition includes background, i.e. events with few protons with $p_p < 300$ MeV/c, neutron at any momenta, pions with $p_\pi < 70$ MeV/c. This background is estimated from Monte Carlo simulation (model dependent).

⋆ Only 410 (CC1p0$\pi$) candidate events were selected, background is about 12% and systematic errors is 20%.
⋆ The semiexclusive NCE scattering

$$\nu_\mu + {}^{40}Ar \rightarrow \nu_\mu + p + B,$$

A subset of this interaction includes signal events with a detected one proton with $\mathbf{p}_p > 300$ MeV/c and no other particles (NC1p) in the final state. There are only preliminary data L.Ren NuFAct2021, 205 (2022)

⋆ For CC1p0$\pi$ events the flux-integrated differential cross sections in muon and proton momenta and angles are defined as

$$\langle d\sigma/dx\rangle = \int_{\varepsilon_{min}}^{\varepsilon_{max}} W_\nu(\varepsilon_\nu) d\sigma/dx(x,\varepsilon_\nu) d\varepsilon_\nu,$$

where $W_\nu$ is the unit-normalized neutrino flux, and neutrino flux $I_\nu$ has maximum at $\varepsilon_\nu \approx 0.7$ GeV in the range of neutrino energy $0.2 < \varepsilon_\nu < 3$ GeV.

$$W_\nu(\varepsilon_\nu) = I_\nu(\varepsilon_\nu)/\Phi, \quad \Phi = \int_{\varepsilon_{min}}^{\varepsilon_{max}} I_\nu(\varepsilon_\nu) d\varepsilon_\nu$$

⋆ The differential flux-integrated cross sections depend upon the shape of the neutrino flux. The cross sections measured at near and far detectors can be different due to neutrino oscillation effects.

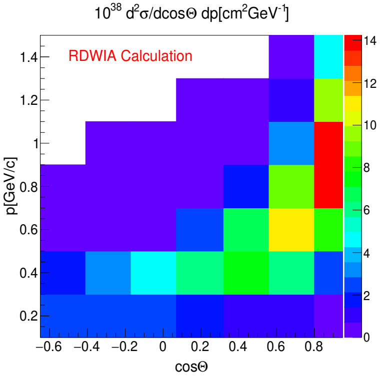


The flux-integrated double-differential cross section of $^{40}$Ar$(\nu_\mu, \mu p)$ neutrino scattering $d^2\sigma/dp_\mu d\cos\theta$ calculated within the RDWIA with $M_A = 1$ GeV as a function of muon momentum $\mathbf{p}_\mu$ and muon scattering angle $\cos\theta$. The maximum of the calculated cross section is in the range $0.7 < p_\mu < 1.1$ GeV/c and $0.8 < \cos\theta < 0.96$. So, neutrino interactions with energy higher then 1 GeV and high values of $\cos\theta$, yield the main contribution to the measured cross sections.

A.Butkevich, PRC 105, 025501 (2021)

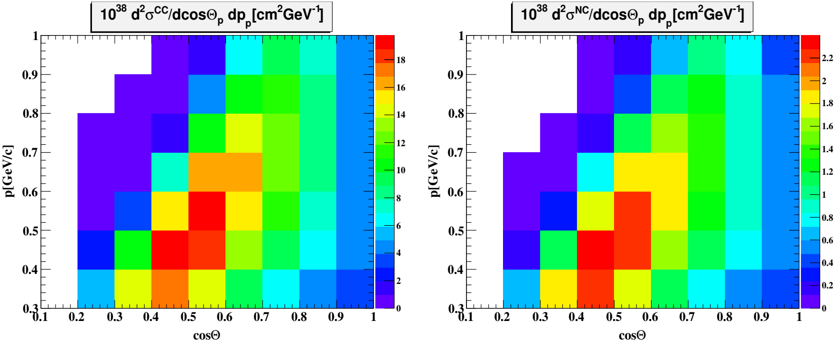


The flux-integrated double-differential cross sections $d^2\sigma/dp_p d\cos\theta_p$ of the semiexclusive CCQE (left panel) and NCE (right panel) of $\nu_\mu$-Ar scattering as functions of proton momentum and scattering angle. Here the results were obtained within the RDWIA with the value of $M_A = 1$ GeV and $\Delta s = 0$. Tne maximum of the calculated cross sections is in the region $0.3 < p_p < 0.6$ GeV/c and $0.4 < \cos\theta_p < 0.6$ ($\theta_p = 60^\circ$)

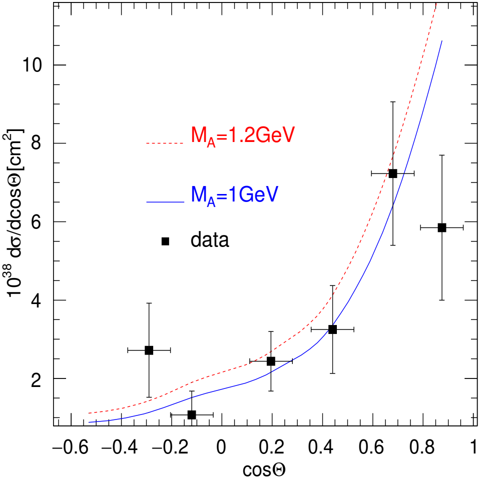


The flux-integrated differential $d\sigma/d\cos\theta$ as a function of measured muon scattering angle. Error bars show the total (statistical and systematic) uncertainty at $1\sigma$ confidence level. MicroBooNE: P.Abratenko et al. PRD 105, 072001 (2022). The data are compared to the RDWIA calculations with the values of $M_A = 1$ GeV and 1.2 GeV. Calculated cross sections are in overall agreement with data, except for the highest $\cos\theta$ bin.

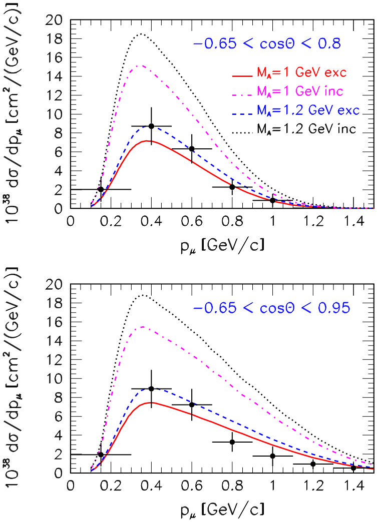


The measured flux-integrated differential $d\sigma/dp_\mu$ cross section for $-0.65 < \cos\theta < 0.95$ and $-0.65 < \cos\theta < 0.8$ as a function of muon momentum MicroBooNE: P.Abratenko et al. PRD 105,072001 (2022). The calculated with $M_A = 1$ GeV and 1.2 GeV semiexclusive and inclusive cross sections are shown as well in this figure. The contribution of $(\nu_\mu, \mu p)$ channel with $p_\mu > 300$ MeV/c to the inclusive $d\sigma/dp_\mu$ cross section increases slowly from 35% at $p_\mu \approx 0.2$ GeV/c to 50% at $p_\mu \approx 0.4$ GeV/c.

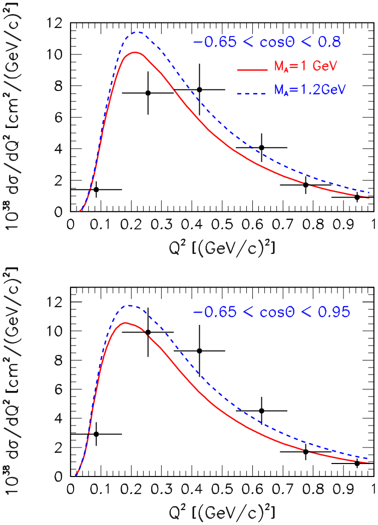


The flux-integrated differential $d\sigma/dQ^2$ cross section as a function of $Q^2$ for $-0.65 < \cos\theta_\mu < 0.95$ и $-0.65 < \cos\theta_\mu < 0.8$. The data MicroBooNE: P.Abratenko et al. PRD 105 are compared to the RDWIA calculation *A.Butkevich, PRC 105, 025501 (2022)* with $M_A = 1$ and $1.2$ GeV. At low $Q^2 < 0.3$ (GeV/c)$^2$ the cross section depends weakly on the value of axial mass and $Q^2$ distribution is controled by nuclear effects.

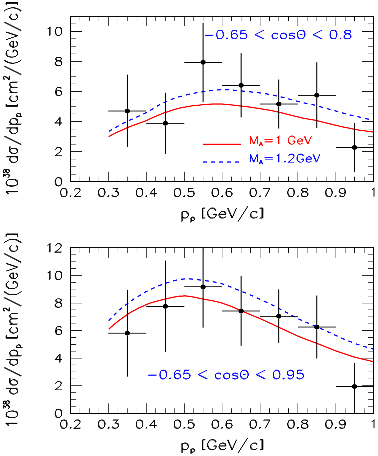


The flux-integrated differential $d\sigma/dp_p$ cross section as a function of proton momentum. The cross section is shown for $\cos\theta < 0.8$ (top) and $\cos\theta > 0.8$ (bottom). Also shown are results obtained in the RDWIA with $M_A = 1$ GeV and 1.2 GeV. The measured proton momentum distribution is wider than the muon momentum distribution and the maximum of the $d\sigma/dp_p$ cross section is located at $p_p \approx 0.5$ GeV.

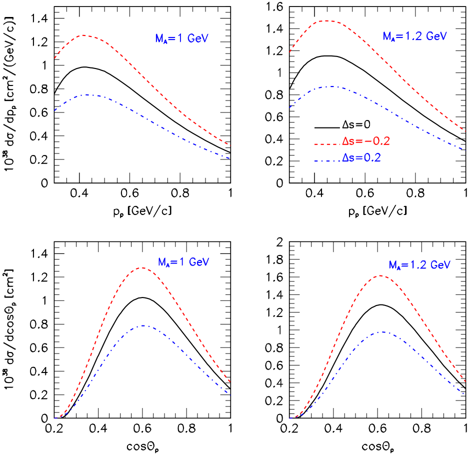


The flux-integrated differential $d\sigma^{(nc)}/dp_p$ cross section as a function of proton momentum (upper panel) and $d\sigma^{(nc)}/d\cos\theta_p$ (lower panel) as a function of $\cos\theta_p$ calculated with axial mass 1 and 1.2 GeV. Also shown is the strange quark effect on the NCE cross section with values of $\Delta s = -0.2, 0, 0.2$. The cross sections decrease when increasing $\Delta s$, by about 65% when $\Delta s$ running from $\Delta s = -0.2$ to $\Delta s = 0.2$. Theoretical uncertainties on the $d\sigma^{(nc)}/dQ^2$ cross section due to uncertainties of the values of $M_A$ and $\Delta s$ can reach 75%.

⋆ In the LArTPC detector momenta of stopped muon and proton can be reconstructed with accuracy 2-3%. For CCQE and NCE two-body interactions the neutrino energy can be determed from the final state lepton/proton energy and angle or using the calorimetric method.

⋆ The incoming neutrino energy can be determing (ignore the Fermi nucleon motion and nuclear effects) in the following way

$$\varepsilon^{l}_{rec} = \frac{\varepsilon_f(m-\epsilon_b) - (\epsilon_b^2 + m_l^2 - 2m\epsilon_b)/2}{(m-\epsilon_b) - \varepsilon_f + k_f\cos\theta}$$

$$\varepsilon^{p}_{rec} = \frac{T_p(m-\epsilon_b) - (m_l^2 - \epsilon_b^2)/2}{p_x\cos\theta_p - (T_p+\epsilon_b)} \quad CCQE\ and\ NCE$$

$$\varepsilon^{lp}_{rec} = E_\mu + T_p + \epsilon_b,$$

where $m_l$ is mass of lepton, $T_p$ is nucleon kinetic energy and $\varepsilon_b$ is nucleon binding energy.

⋆ For the NCE scattering to reconstruct the incoming neutrino energy the kinematic of the outgoing proton is used.

⋆ The differential cross section as a function of proton momentum and reconstructed neutrino energy $\varepsilon^{p}_{rec}$ can be written as

$$\frac{d^2\sigma}{dp_x d\varepsilon^{p}_{rec}} = R_{\varepsilon_p}\frac{d^2\sigma}{dp_x d\cos\theta_p},$$

где $R_{\varepsilon_p} = [p_x^2 + m_l^2 - (T_x + \epsilon_b)]/[2p_x(\varepsilon^{p}_{rec})^2]$.

⋆ The differential cross section as a function of the reconstructed neutrino energy

$$\frac{d\sigma}{d\varepsilon^{p}_{rec}} = \int_{p_{min}}^{p_{max}} \frac{d^2\sigma}{d\varepsilon^{p}_{rec} dp_x} dp_x$$

can be measured in experiments (in the MicroBooNE experiment) $p_{min} = 0.3$ GeV/c and $p_{max} = 1$ GeV/c).

⋆ In the SBN program three detectors are used to measure the same neutrino beam at differen distance from source. The location of the near SBND and far ICARUS-T600 detectors are optimized for maximal sensitivity in search for $m_4 \sim 1$ eV.

⋆ The flux-integrated neutrino cross section $d\sigma/d\varepsilon^p_{rec}$ at the near detector (with no-oscillation) has form

$$\left(\frac{d\sigma^{(cc)(nc)}}{d\varepsilon^p_{rec}}\right)_{near} = \int W_\nu(\varepsilon_i)\frac{d\sigma^{(cc)(nc)}}{d\varepsilon^p_{rec}}(\varepsilon_i,\varepsilon^p_{rec})d\varepsilon^p_i.$$

⋆ The flux-integrated neutrino cross sections at the far detector with oscillation effects can be written as

$$\left(\frac{d\sigma^{(cc)(nc)}}{\varepsilon^p_{rec}}\right)^{osc}_{far} = \int W_\nu(\varepsilon_i)P^{(cc)(nc)}_{(\nu_\mu\nu_\mu)(\nu s)}(\varepsilon_i)\frac{d\sigma^{(cc)(nc)}}{d\varepsilon^p_{rec}}(\varepsilon_i,\varepsilon^p_{rec})d\varepsilon_i,$$

where $P^{cc}_{\nu_\mu\nu_\mu}$ and $P^{nc}_{\nu_s}$ are probabilities of survival of muon and active neutrinos, respectively.

⋆ The ratio

$$R_\sigma(\varepsilon^p_{rec}) = \left(d\sigma^{(cc)(nc)}/d\varepsilon^p_{rec}\right)^{osc}_{far} \Big/ \left(d\sigma^{(cc)(nc)}/d\varepsilon^p_{rec}\right)_{near}$$

can be used to determine significance of the muon and active neutrinos disappearance observed at the far detector.

⋆ The uncertainties in the neutrino flux and neutrino cross sections (10-30%) are cancelated.

⋆ We use 3+1 neutrino framework and assuming that $m_4 >> m_3, m_2, m_1$. The short-baseline survival probability of $\nu_\mu$ and $\nu_{active}$ at the short distance $L \sim E/\Delta m^2_{41}$ takes form

$$P_{\nu_\mu \nu_\mu} = 1 - \sin^2\theta_{\mu\mu} \sin^2\Delta_{41} \quad for \quad \nu_\mu$$
$$P_{\nu s} = 1 - \sin^2\theta_{\mu s} \sin^2\Delta_{41} \quad for \quad active \quad \nu$$

where $\Delta_{41} = \Delta m^2_{41} L/4E$ and $\theta_{\alpha i}$ are effective mixing angle.
⋆ These angles are expressed in terms of matrix elements of 4×4 PMNS matrix as

$$\sin^2 2\theta_{\mu\mu} = 4(1 - |U_{\mu 4}|^2)|U_{\mu 4}|^2$$
$$\sin^2 2\theta_{\mu s} = 4|U_{\mu 4}|^2 |U_{s4}|^2$$

$$|U_{\mu 4}|^2 = [1 - (1 - \sin^2 2\theta_{\mu\mu})^{1/2}]/2$$
$$|U_{s4}|^2 = \sin^2 2\theta_{\mu s}/4|U_{\mu 4}|^2 \quad admixture \quad of \quad mass \ state \ \nu_4 \ in \ \nu_s$$

⋆ From unitarity of PMNS matrix $\sum |U_{i4}|^2 = 1$, it follows that

$$\sin^2 2\theta_{\mu s} = \sin^2 2\theta_{\mu\mu} - \sin^2 2\theta_{\mu e} - \sin^2 2\theta_{\mu\tau}$$

and $\sin^2 2\theta_{\mu\mu} > \sin^2 2\theta_{\mu s}$.
⋆ Allowed values of $(\Delta m^2_{41}, \sin^2 2\theta_{\mu\mu})$ were found in the MicroBooNE experiment MicroBooNE Note 1106: $1 \leq \Delta m^2_{14} \leq 5$ eV$^2$, $0.09 \leq \sin^2 2\theta_{\mu\mu} \leq 0.25$. There are no data about value of $\theta_{\mu s}$. We estimate allowed values of $\sin 2\theta_{\mu s}$ as $0.085 \leq \sin^2 2\theta_{\mu s} \leq 0.245$.

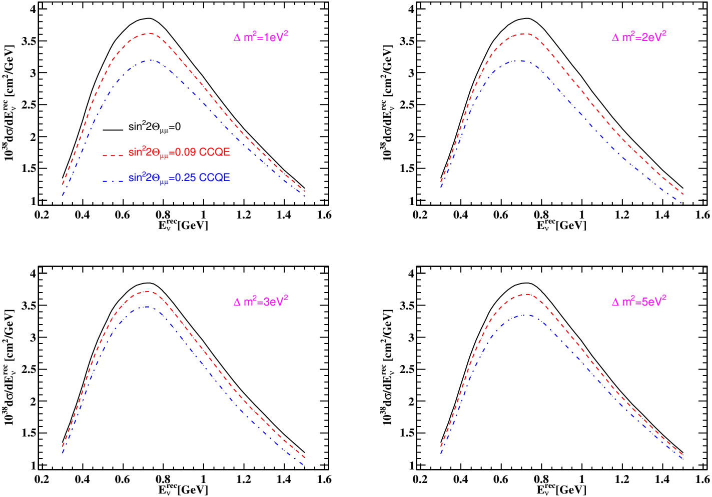


The flux-integrated semiexclusive CCQE cross section as a function of $E_\nu^{rec} = \varepsilon_{rec}$. The results were obtained with $M_A = 1$ GeV without ($\sin^2 2\theta_{\mu\mu} = 0$) and with oscillation effects for the four values $\Delta m^2_{41} = 1, 2, 3, 5$ eV$^2$ and $\sin^2 2\theta_{\mu\mu} = 0.05, 0.25$. The far detector is located at the distance $L = 600$ m.

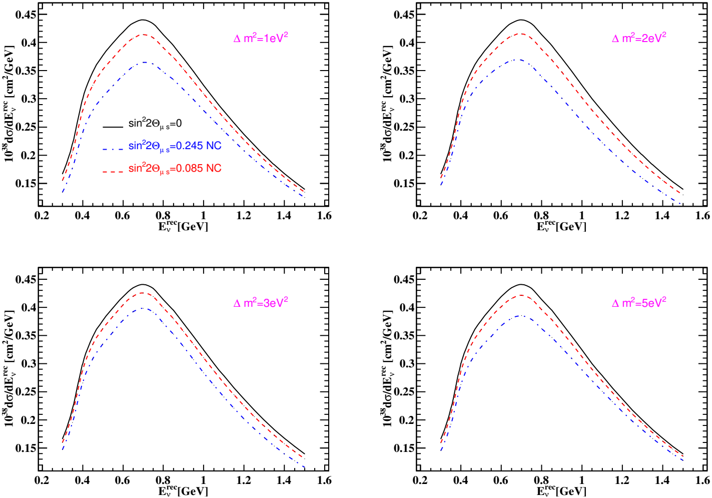


The flux-integrated semiexclusive NCE cross section as a function of $E_\nu^{rec}$ The results were obtained with $M_A = 1$ GeV and $\Delta s = 0$ without ($\sin^2 2\theta_{\mu\mu} = 0$) and with oscillation effects for the four values $\Delta m^2_{41} = 1, 2, 3, 5$ eV$^2$ and distance $L = 600$ m.

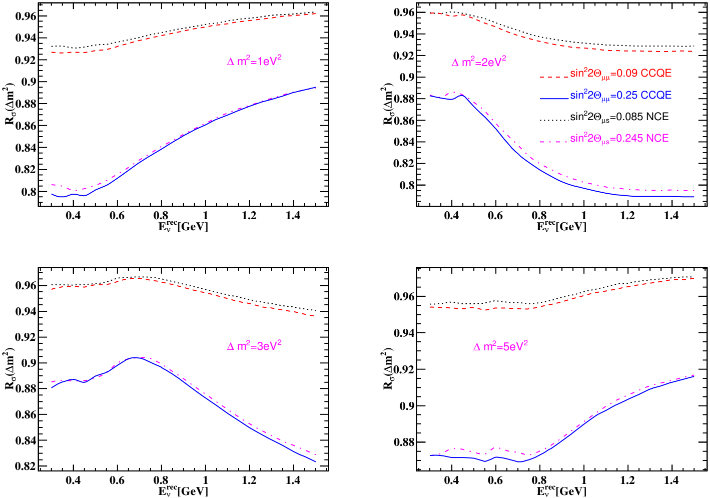


The ratios $R_\sigma = far/near$ for the flux-integrated semiexclusive CCQE and NCE cross sections as functions of $E_\nu^{rec}$. The shape of the $R_\sigma(E_\nu^{rec})$ function depends on the value of $\Delta m^2_{41}$. This ratio is sensitive to the oscillation parameters.

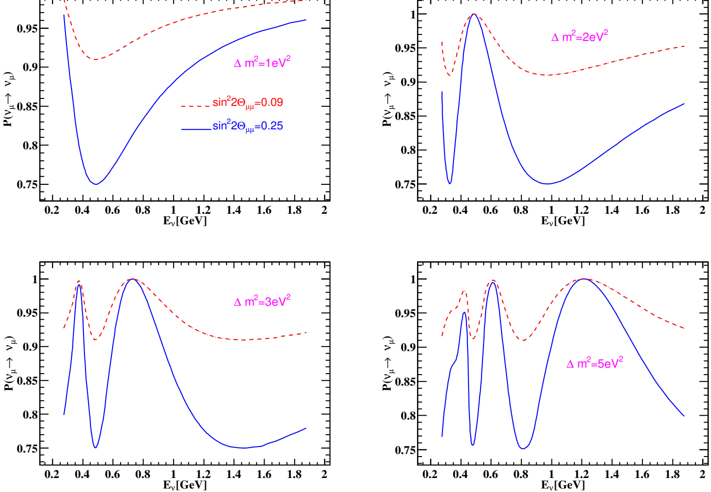


The survival probability for muon neutrino $P_{\nu_\mu \nu_\mu}$ at the distance $L = 600$ m, calculated for $\Delta m^2_{41} = 1, 2, 3, 5$ eV$^2$ and $\sin^2 2\theta_{\mu\mu} = 0.05, 0.25$. The position of the minimum $\varepsilon^{rec}_{min}$ and maximum $\varepsilon^{rec}_{max}$ in the $R_\sigma(E^{rec}_\nu)$ distribution correlates strongly with energy, that corresponds to the first minimum $E_{min} = 2.57\Delta m_{41} L/\pi$ and maximum $E_{max} = E_{min}/2$ in the $P_{\nu_\mu \nu_\mu}(\varepsilon_\nu)$. For example, $E^{rec}_{min}(E_{min}) \approx 0.45(0.48)$ GeV at $\Delta m^2_{41} = 1$ eV$^2$.

# Conclusion

- ⋆ We calculated the semiexclusive CCQE and NCE cross sections of neutrino scattering on $^{40}$Ar with $M_A = 1$ and $1.2$ GeV.
- ⋆ The elastic scattering cross sections are evaluated with different strange quark distributions $\Delta s = -0.2, 0, 0.2$ to the NC axial form factor. The theoretical unsertanties in the NCE cross sections due to unsertanties in the axial form factor (in $M_A$ and $\Delta s$) can reach 75%.
- ⋆ The BNB flux-integrated differential CCQE and NCE cross sections as functions of the reconstaructed neutrino energy are calculated for the far detector of the SBN experiment with no-oscillation and taking into account the short baseline sterile neutrino oscillation effects leading to disappearence of $\nu_\mu$ and $\nu_{active}$. The 3+1 model with values of oscillation parameters $1 \leq \Delta m^2_{41} \leq 5$ eV$^2$ and $0.09(0.085) \leq \sin^2 2\theta_{\mu\mu(\nu s)} \leq 0.25(0.245)$ were used.

# Conclusion

- ⋆ To show the oscillation effect the $R_\sigma$ ratio of the cross sections predicted at the far and near detectors were calculated. The shape and position of the minimum and maximum of the $R_\sigma$ ratio depend on the value of $\Delta m^2_{41}$ and correlate with the position of the first minimum and maximum in the survival probability for muon and active neutrino at the far detector.
- ⋆ The ratio $R_\sigma(E_{rec})$ can be used in a light sterile neutrino search in the short baseline neutrino experiments.

# BACKUP

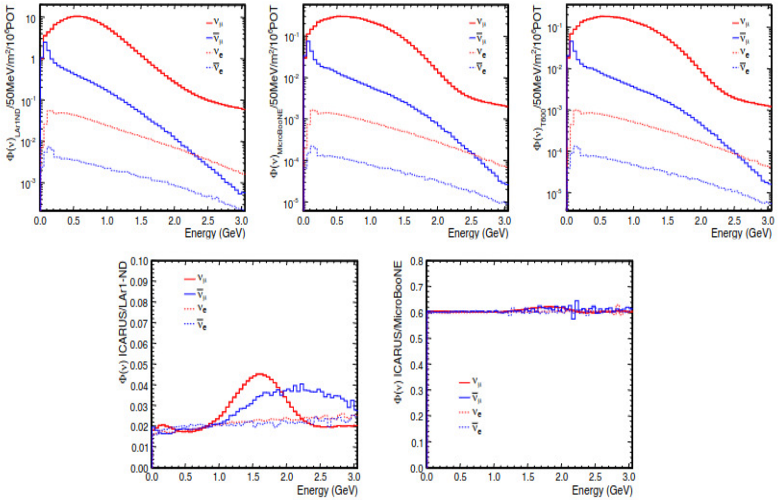


(Top) The BNB flux at the three SBN detectors: (left) SBND, (center) MicroBooNE, and (right) ICARUS-T600. (Bottom) Ratio of the fluxes for each neutrino species between ICARUS and SBND (left) and ICARUS and MicroBooNE (right). The composition of the flux in neutrino mode: $\nu_\mu$: 93.65%, $\bar{\nu}_\mu$: 5.79%, $\nu_e$: 0.51%,$\bar{\nu}_e$: 0.06%.

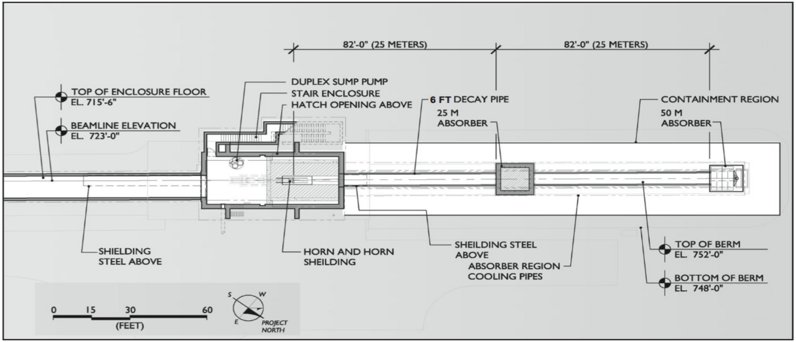


Schematic drawing of BNB including the 8 GeV extracting line, target hall and 50 m decay region.

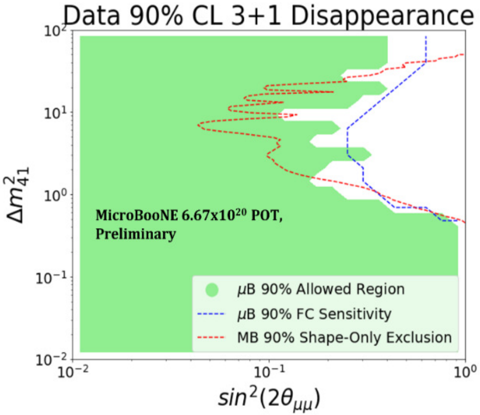


The MicroBooNE allowed region of 3+1 model phase space in gree, and the excluded region in the white with sensitivity overlaid in blue.